

FFT procedures of size  $N$ , and thus requires a total of  $O(N^2 \log_2 N)$  operations. Figure 4.3 is computed with this algorithm.

**Inverse Transform** The following theorem discretizes the reconstruction formula and the energy conservation of Theorem 4.1.

**Theorem 4.2** *If  $f$  is a signal of period  $N$  then*

$$f[n] = \frac{1}{N} \sum_{m=0}^{N-1} \sum_{l=0}^{N-1} Sf[m, l] g[n-m] \exp\left(\frac{i2\pi ln}{N}\right) \quad (4.28)$$

and

$$\sum_{n=0}^{N-1} |f[n]|^2 = \frac{1}{N} \sum_{l=0}^{N-1} \sum_{m=0}^{N-1} |Sf[m, l]|^2. \quad (4.29)$$

This theorem is proved by applying the Parseval and Plancherel formulas of the discrete Fourier transform, exactly as in the proof of Theorem 4.1. The reconstruction formula (4.28) is rewritten

$$f[n] = \frac{1}{N} \sum_{m=0}^{N-1} g[n-m] \sum_{l=0}^{N-1} Sf[m, l] \exp\left(\frac{i2\pi ln}{N}\right).$$

The second sum computes for each  $0 \leq m < N$  the inverse discrete Fourier transform of  $Sf[m, l]$  with respect to  $l$ . This is calculated with  $N$  FFT procedures, requiring a total of  $O(N^2 \log_2 N)$  operations.

A discrete windowed Fourier transform is an  $N^2$  image  $Sf[l, m]$  that is very redundant, since it is entirely specified by a signal  $f$  of size  $N$ . The redundancy is characterized by a discrete reproducing kernel equation, which is the discrete equivalent of (4.20).

### 4.3 Wavelet Transforms <sup>1</sup>

To analyze signal structures of very different sizes, it is necessary to use time-frequency atoms with different time supports. The wavelet

transform decomposes signals over dilated and translated wavelets. A wavelet is a function  $\psi \in \mathbf{L}^2(\mathbb{R})$  with a zero average:

$$\int_{-\infty}^{+\infty} \psi(t) dt = 0. \quad (4.30)$$

It is normalized  $\|\psi\| = 1$ , and centered in the neighborhood of  $t = 0$ . A family of time-frequency atoms is obtained by scaling  $\psi$  by  $s$  and translating it by  $u$ :

$$\psi_{u,s}(t) = \frac{1}{\sqrt{s}} \psi\left(\frac{t-u}{s}\right).$$

These atoms remain normalized:  $\|\psi_{u,s}\| = 1$ . The wavelet transform of  $f \in \mathbf{L}^2(\mathbb{R})$  at time  $u$  and scale  $s$  is

$$Wf(u, s) = \langle f, \psi_{u,s} \rangle = \int_{-\infty}^{+\infty} f(t) \frac{1}{\sqrt{s}} \psi^*\left(\frac{t-u}{s}\right) dt. \quad (4.31)$$

**Linear Filtering** The wavelet transform can be rewritten as a convolution product:

$$Wf(u, s) = \int_{-\infty}^{+\infty} f(t) \frac{1}{\sqrt{s}} \psi^*\left(\frac{t-u}{s}\right) dt = f \star \bar{\psi}_s(u) \quad (4.32)$$

with

$$\bar{\psi}_s(t) = \frac{1}{\sqrt{s}} \psi^*\left(\frac{-t}{s}\right).$$

The Fourier transform of  $\bar{\psi}_s(t)$  is

$$\widehat{\bar{\psi}}_s(\omega) = \sqrt{s} \hat{\psi}^*(s\omega). \quad (4.33)$$

Since  $\hat{\psi}(0) = \int_{-\infty}^{+\infty} \psi(t) dt = 0$ , it appears that  $\hat{\psi}$  is the transfer function of a band-pass filter. The convolution (4.32) computes the wavelet transform with dilated band-pass filters.

**Analytic Versus Real Wavelets** Like a windowed Fourier transform, a wavelet transform can measure the time evolution of frequency transients. This requires using a complex analytic wavelet, which can

separate amplitude and phase components. The properties of this analytic wavelet transform are described in Section 4.3.2, and its application to the measurement of instantaneous frequencies is explained in Section 4.4.2. In contrast, real wavelets are often used to detect sharp signal transitions. Section 4.3.1 introduces elementary properties of real wavelets, which are developed in Chapter 6.

### 4.3.1 Real Wavelets

Suppose that  $\psi$  is a real wavelet. Since it has a zero average, the wavelet integral

$$Wf(u, s) = \int_{-\infty}^{+\infty} f(t) \frac{1}{\sqrt{s}} \psi^* \left( \frac{t-u}{s} \right) dt$$

measures the variation of  $f$  in a neighborhood of  $u$ , whose size is proportional to  $s$ . Section 6.1.3 proves that when the scale  $s$  goes to zero, the decay of the wavelet coefficients characterizes the regularity of  $f$  in the neighborhood of  $u$ . This has important applications for detecting transients and analyzing fractals. This section concentrates on the completeness and redundancy properties of real wavelet transforms.

**Example 4.6** Wavelets equal to the second derivative of a Gaussian are called *Mexican hats*. They were first used in computer vision to detect multiscale edges [354]. The normalized Mexican hat wavelet is

$$\psi(t) = \frac{2}{\pi^{1/4} \sqrt{3\sigma}} \left( \frac{t^2}{\sigma^2} - 1 \right) \exp \left( \frac{-t^2}{2\sigma^2} \right). \quad (4.34)$$

For  $\sigma = 1$ , Figure 4.6 plots  $-\psi$  and its Fourier transform

$$\hat{\psi}(\omega) = \frac{-\sqrt{8} \sigma^{5/2} \pi^{1/4}}{\sqrt{3}} \omega^2 \exp \left( \frac{-\sigma^2 \omega^2}{2} \right). \quad (4.35)$$

Figure 4.7 shows the wavelet transform of a signal that is piecewise regular on the left and almost everywhere singular on the right. The maximum scale is smaller than 1 because the support of  $f$  is normalized to  $[0, 1]$ . The minimum scale is limited by the sampling interval of the discretized signal used in numerical calculations. When the scale

decreases, the wavelet transform has a rapid decay to zero in the regions where the signal is regular. The isolated singularities on the left create cones of large amplitude wavelet coefficients that converge to the locations of the singularities. This is further explained in Chapter 6.

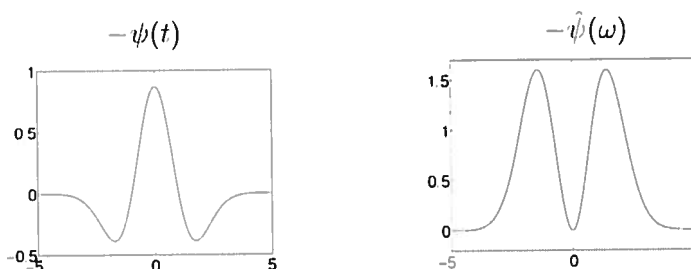


Figure 4.6: Mexican hat wavelet (4.34) for  $\sigma = 1$  and its Fourier transform.

A real wavelet transform is complete and maintains an energy conservation, as long as the wavelet satisfies a weak admissibility condition, specified by the following theorem. This theorem was first proved in 1964 by the mathematician Calderón [111], from a different point of view. Wavelets did not appear as such, but Calderón defines a wavelet transform as a convolution operator that decomposes the identity. Grossmann and Morlet [200] were not aware of Calderón's work when they proved the same formula for signal processing.

**Theorem 4.3 (Calderón, Grossmann, Morlet)** *Let  $\psi \in L^2(\mathbb{R})$  be a real function such that*

$$C_\psi = \int_0^{+\infty} \frac{|\hat{\psi}(\omega)|^2}{\omega} d\omega < +\infty. \quad (4.36)$$

*Any  $f \in L^2(\mathbb{R})$  satisfies*

$$f(t) = \frac{1}{C_\psi} \int_0^{+\infty} \int_{-\infty}^{+\infty} Wf(u, s) \frac{1}{\sqrt{s}} \psi\left(\frac{t-u}{s}\right) du \frac{ds}{s^2}, \quad (4.37)$$

*and*

$$\int_{-\infty}^{+\infty} |f(t)|^2 dt = \frac{1}{C_\psi} \int_0^{+\infty} \int_{-\infty}^{+\infty} |Wf(u, s)|^2 du \frac{ds}{s^2}. \quad (4.38)$$

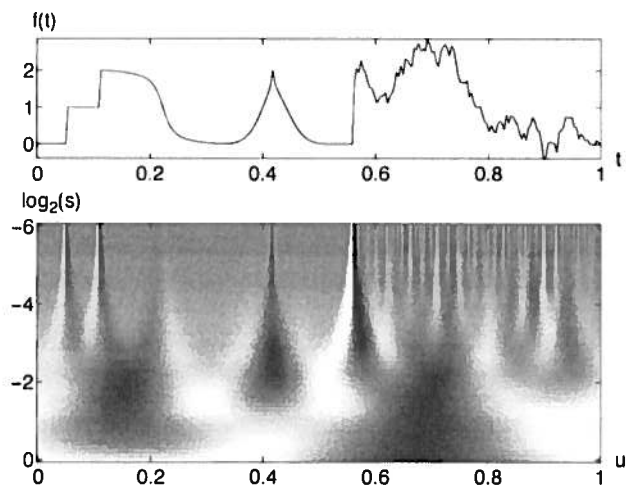


Figure 4.7: Real wavelet transform  $Wf(u, s)$  computed with a Mexican hat wavelet (4.34). The vertical axis represents  $\log_2 s$ . Black, grey and white points correspond respectively to positive, zero and negative wavelet coefficients.

*Proof*<sup>1</sup>. The proof of (4.38) is almost identical to the proof of (4.18). Let us concentrate on the proof of (4.37). The right integral  $b(t)$  of (4.37) can be rewritten as a sum of convolutions. Inserting  $Wf(u, s) = f \star \bar{\psi}_s(u)$  with  $\psi_s(t) = s^{-1/2} \psi(t/s)$  yields

$$\begin{aligned} b(t) &= \frac{1}{C_\psi} \int_0^{+\infty} Wf(\cdot, s) \star \psi_s(t) \frac{ds}{s^2} \\ &= \frac{1}{C_\psi} \int_0^{+\infty} f \star \bar{\psi}_s \star \psi_s(t) \frac{ds}{s^2}. \end{aligned} \quad (4.39)$$

The “ $\cdot$ ” indicates the variable over which the convolution is calculated. We prove that  $b = f$  by showing that their Fourier transforms are equal. The Fourier transform of  $b$  is

$$\hat{b}(\omega) = \frac{1}{C_\psi} \int_0^{+\infty} \hat{f}(\omega) \sqrt{s} \hat{\psi}^*(s\omega) \sqrt{s} \hat{\psi}(s\omega) \frac{ds}{s^2} = \frac{\hat{f}(\omega)}{C_\psi} \int_0^{+\infty} |\hat{\psi}(s\omega)|^2 \frac{ds}{s}.$$

Since  $\psi$  is real we know that  $|\hat{\psi}(-\omega)|^2 = |\hat{\psi}(\omega)|^2$ . The change of variable  $\xi = s\omega$  thus proves that

$$\hat{b}(\omega) = \frac{1}{C_\psi} \hat{f}(\omega) \int_0^{+\infty} \frac{|\hat{\psi}(\xi)|^2}{\xi} d\xi = \hat{f}(\omega). \quad (4.39)$$

The theorem hypothesis

$$C_\psi = \int_0^{+\infty} \frac{|\hat{\psi}(\omega)|^2}{\omega} d\omega < +\infty$$

is called the wavelet *admissibility condition*. To guarantee that this integral is finite we must ensure that  $\hat{\psi}(0) = 0$ , which explains why we imposed that wavelets must have a zero average. This condition is nearly sufficient. If  $\hat{\psi}(0) = 0$  and  $\hat{\psi}(\omega)$  is continuously differentiable then the admissibility condition is satisfied. One can verify that  $\hat{\psi}(\omega)$  is continuously differentiable if  $\psi$  has a sufficient time decay

$$\int_{-\infty}^{+\infty} (1 + |t|) |\psi(t)| dt < +\infty.$$

**Reproducing Kernel** Like a windowed Fourier transform, a wavelet transform is a redundant representation, whose redundancy is characterized by a reproducing kernel equation. Inserting the reconstruction formula (4.37) into the definition of the wavelet transform yields

$$Wf(u_0, s_0) = \int_{-\infty}^{+\infty} \left( \frac{1}{C_\psi} \int_0^{+\infty} \int_{-\infty}^{+\infty} Wf(u, s) \psi_{u,s}(t) du \frac{ds}{s^2} \right) \psi_{u_0, s_0}^*(t) dt.$$

Interchanging these integrals gives

$$Wf(u_0, s_0) = \frac{1}{C_\psi} \int_{-\infty}^{+\infty} K(u, u_0, s, s_0) Wf(u, s) du \frac{ds}{s^2}, \quad (4.40)$$

with

$$K(u_0, u, s_0, s) = \langle \psi_{u,s}, \psi_{u_0, s_0} \rangle. \quad (4.41)$$

The reproducing kernel  $K(u_0, u, s_0, s)$  measures the correlation of two wavelets  $\psi_{u,s}$  and  $\psi_{u_0, s_0}$ . The reader can verify that any function  $\Phi(u, s)$  is the wavelet transform of some  $f \in \mathbf{L}^2(\mathbb{R})$  if and only if it satisfies the reproducing kernel equation (4.40).

**Scaling Function** When  $Wf(u, s)$  is known only for  $s < s_0$ , to recover  $f$  we need a complement of information corresponding to  $Wf(u, s)$  for  $s > s_0$ . This is obtained by introducing a *scaling function*  $\phi$  that is an aggregation of wavelets at scales larger than 1. The modulus of its Fourier transform is defined by

$$|\hat{\phi}(\omega)|^2 = \int_1^{+\infty} |\hat{\psi}(s\omega)|^2 \frac{ds}{s} = \int_\omega^{+\infty} \frac{|\hat{\psi}(\xi)|^2}{\xi} d\xi, \quad (4.42)$$

and the complex phase of  $\hat{\phi}(\omega)$  can be arbitrarily chosen. One can verify that  $\|\phi\| = 1$  and we derive from the admissibility condition (4.36) that

$$\lim_{\omega \rightarrow 0} |\hat{\phi}(\omega)|^2 = C_\psi. \quad (4.43)$$

The scaling function can thus be interpreted as the impulse response of a low-pass filter. Let us denote

$$\phi_s(t) = \frac{1}{\sqrt{s}} \phi\left(\frac{t}{s}\right) \quad \text{and} \quad \bar{\phi}_s(t) = \phi_s^*(-t).$$

The low-frequency approximation of  $f$  at the scale  $s$  is

$$Lf(u, s) = \left\langle f(t), \frac{1}{\sqrt{s}} \phi \left( \frac{t-u}{s} \right) \right\rangle = f \star \bar{\phi}_s(u). \quad (4.44)$$

With a minor modification of the proof of Theorem 4.3, it can be shown that

$$f(t) = \frac{1}{C_\psi} \int_0^{s_0} Wf(\cdot, s) \star \psi_s(t) \frac{ds}{s^2} + \frac{1}{C_\psi s_0} Lf(\cdot, s_0) \star \phi_{s_0}(t). \quad (4.45)$$

**Example 4.7** If  $\psi$  is the second order derivative of a Gaussian whose Fourier transform is given by (4.35), then the integration (4.42) yields

$$\hat{\phi}(\omega) = \frac{2\sigma^{3/2}\pi^{1/4}}{\sqrt{3}} \sqrt{\omega^2 + \frac{1}{\sigma^2}} \exp\left(-\frac{\sigma^2\omega^2}{2}\right). \quad (4.46)$$

Figure 4.8 displays  $\phi$  and  $\hat{\phi}$  for  $\sigma = 1$ .

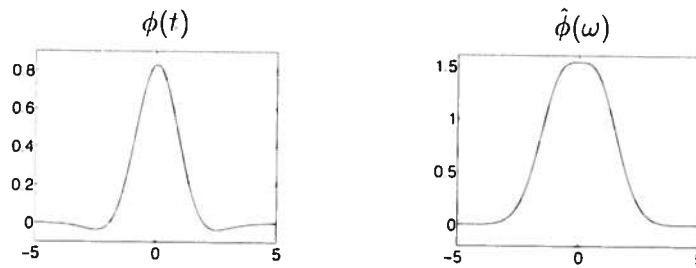


Figure 4.8: Scaling function associated to a Mexican hat wavelet and its Fourier transform calculated with (4.46).

### 4.3.2 Analytic Wavelets

To analyze the time evolution of frequency tones, it is necessary to use an analytic wavelet to separate the phase and amplitude information of signals. The properties of the resulting analytic wavelet transform are studied.